Journal of Cleaner Production 223 (2019) 692–703

Contents lists available at ScienceDirect

Journal of Cleaner Production

journal homepage: www.elsevier.com/locate/jclepro

The swing adsorption reactor cluster for post-combustion CO_2 capture from cement plants

Schalk Cloete [a], Antonio Giuffrida [b], Matteo C. Romano [b], Abdelghafour Zaabout [a, *]

[a] Process Technology Department, SINTEF Industry, Trondheim, Norway
[b] Department of Energy, Politecnico di Milano, Milan, Italy

ARTICLE INFO

Article history:
Received 13 December 2018
Received in revised form
18 February 2019
Accepted 11 March 2019
Available online 13 March 2019

Keywords:
Adsorption-based CO_2 capture
Energy penalty
Cement
Industrial emissions
CCS retrofit

ABSTRACT

The swing adsorption reactor cluster is a promising new method for post-combustion CO_2 capture using a synergistic combination of temperature and pressure swings. The pressure swing is carried out by a vacuum pump and allows for 90% CO_2 capture using only a small temperature swing, which is carried out by a heat pump. The small temperature swing allows the heat pump to transfer heat from carbonation to regeneration at a very high efficiency, minimizing the energy penalty. When applied to a cement plant, the energy penalty reduces further relative to a coal power plant that has a lower CO_2 content in the flue gas. Higher CO_2 concentrations allow a given CO_2 capture ratio to be achieved with a smaller temperature swing, thus further improving the heat pump efficiency. As a result of the high heat pump efficiency and of the limited amount of waste heat available, heat integration with the cement plant yielded negligible efficiency gains. A swing adsorption reactor cluster post-combustion CO_2 capture facility can therefore be constructed independently from the cement plant, making it attractive for retrofits. The specific energy consumption for CO_2 avoidance of the process was determined as 2.04 MJ_{LHV}/kg_{CO2} when using electricity from the average European power mix, which is lower than all competing technologies recently assessed in the literature aside from oxyfuel CO_2 capture. Primary energy consumption will continue to decline as the electricity sector decarbonizes, increasing the attractiveness of the swing adsorption reactor cluster over coming decades.

1. Introduction

The recently released IPCC special report on 1.5 °C global warming (IPCC, 2018) has once again emphasized the urgency of reducing global CO_2 emissions. Limiting global temperature rise to 1.5 °C or even 2 °C requires rapid and broad emissions reductions from all sectors.

Cement production represents about 8% of global CO_2 emissions (Andrew, 2018). Significant decarbonization of cement production is possible only through CO_2 capture techniques, because most of the CO_2 emissions originate from the calcination of limestone used as raw material in clinker production. Simply transitioning to a clean energy source such as hydrogen or renewables will therefore have a limited effect on CO_2 emissions.

Several post-combustion and oxy-combustion processes have been assessed experimentally and through techno-economic analyses in the recent years (Garcia, 2018). Due to its maturity in the application in other sectors, post-combustion CO_2 capture with monoethanolamine (MEA) is often considered as the benchmark technology for CO_2 capture also in cement plants. However, due to the relatively large heat demand for solvent regeneration, combined with the scarcity of waste heat and the lack of low-pressure steam in cement plants, the installation of boilers or combined heat and power plants for steam generation is needed. This causes poor energy performance (i.e. high specific primary energy consumption for CO_2 avoided – SPECCA (Voldsund et al., 2019)) and economic indicators. Cost of CO_2 avoided between 72 and 215 $/t for MEA-based CO_2 capture in cement plants have been reported based on harmonized literature data in a recent IEAGHG review study (Garcia, 2018). For solvent-based post-combustion capture, the reduction of the heat demand for solvent regeneration is the key driver for improved system performance. For example, a CO_2 avoidance cost reduction of 20% compared to the benchmark MEA system has been recently calculated for an optimized chilled ammonia process (Gardarsdottir et al., 2019).

* Corresponding author. Process Technology Department, SINTEF Industry, S.P. Andersens vei 15 B, 7031, Trondheim, Norway.
E-mail address: abdelghafour.zaabout@sintef.no (A. Zaabout).

https://doi.org/10.1016/j.jclepro.2019.03.109

Oxyfuel combustion represents another option widely assessed for the cement sector. In the recent comparative techno-economic study performed in the framework of the Cemcap project (CEMCAP, 2018), oxyfuel combustion resulted as the technology with the best energy efficiency and economic indicators, with SPECCA below 2 MJ/kg_{CO2} (Voldsund et al., 2019) and cost of CO_2 avoided of 42 $€/t_{CO2}$ (Gardarsdottir et al., 2019). Although a complete oxyfuel cement kiln has not been demonstrated yet, significant experimental work focused on important individual units of the process, such as the pre-calciner (both in lab (Paneru et al., 2018) and in industrially relevant environment (Gimenez et al., 2014)), the main burner (Carrasco et al., 2019) and the clinker cooler (Lino et al., 2018).

Another technology that attracted significant research efforts is Calcium looping (CaL), largely due to the intrinsic advantage of using as CO_2 sorbent the same raw material already used for clinker production. CaL process may be applied in cement kilns according to two fundamental integration options, namely the tail-end configuration, an end of pipe process with limited interactions with the cement kiln (Ozcan et al., 2013), highly suitable for retrofitting (De Lena et al., 2017), and the integrated configuration, where the CaL process is integrated in the cement kiln preheater (Rodríguez et al., 2012). In a recent techno-economic study, cost of CO_2 avoided of 52 and 58 $€/t_{CO2}$ have been estimated for the tail-end and the more immature integrated configurations, respectively (De Lena et al., 2019). From the experimental side, recent tests have demonstrated the tail-end CaL process for cement plants with fluidized bed reactors (Arias et al., 2017) up to TRL 5 (Hornberger et al., 2017) and assessed the fundamentals of the integrated CaL process with entrained-flow reactors using the raw meal as CO_2 sorbent (Turrado et al., 2018).

A limited number of works have focused on other post-combustion capture systems, such as membranes (Hägg et al., 2017) and low temperature sorbents (Nelson et al., 2014). As for membranes, a recent comparative study showed that costs of CO_2 avoided for membrane assisted liquefaction process (i.e. membrane separation system integrated in the CO_2 compression and purification unit) similar to the benchmark MEA process (Gardarsdottir et al., 2019). It must be remarked that membrane-based CO_2 separation is an electric energy consuming process, while solvent and CaL processes are mainly heat consuming processes (in the form of low-grade heat and fuel respectively). Therefore, the energy and economic performance of membrane-based separation are highly dependent on the power generation technology supporting the CO_2 capture process. As for sorbents, the most significant documented study is related to the RTI sorption technology, based on temperature swing adsorption in dual fluidized circulating reactors (Nelson et al., 2014), where sorbent stability tests and preliminary techno-economic analysis have been performed.

Finally, other studies assessed advanced calcination systems based on indirect heating via high temperature heat carriers (Rodríguez et al., 2008) (also within a CaL process (Diego et al., 2016)) and high temperature heat exchanger (or "direct capture" system) (Hills et al., 2016). Due to the low TRL of such processes, requiring significant modifications of the pre-calciner and the pre-heater system compared to the state-of-the-art technology, reliable economic benchmarking of these processes is intrinsically challenging.

An important feature for any CO_2 capture technology is the simplicity of retrofitting of existing cement kilns. This is particularly important in some world regions such as Europe, where a limited number of new plants is expected to be built in the future. From this point of view, post-combustion capture technologies have some important advantages (Voldsund et al., 2019), namely no impact on the clinker burning process and low shut-down time needed for connecting the cement kiln with the CO_2 capture process (Hills et al., 2016).

This study investigates a new sorption-based technology: the Swing Adsorption Reactor Cluster (SARC) (Zaabout et al., 2017). SARC is a new post-combustion capture concept, utilizing only electricity to capture CO_2 using a synergistic combination of temperature swing with a heat pump and pressure swing with a vacuum pump. For this reason, SARC does not face integration challenges and will also allow for simple retrofitting of existing cement plants.

The SARC concept is illustrated in Fig. 1. It consists of a cluster of dynamically operated fluidized bed reactors cycling through four process steps:

1. Carbonation, where a sorbent adsorbs CO_2 from the cement plant flue gas stream. In the base case in this study, this step takes place at 58 °C and atmospheric pressure.
2. Evacuation, where N_2 is extracted from the reactor and vented to the atmosphere to prevent it from diluting the CO_2 released in the subsequent regeneration step.
3. Regeneration, where the sorbent is regenerated using a combination of temperature increase and pressure decrease. In the base case, this step takes place at 65 °C and 0.1 bar pressure.
4. Cooling, where the bed is cooled and repressurized in preparation for the subsequent carbonation step.

No transfer of sorbent between reactors is necessary in this arrangement, allowing each reactor to be operated as a standalone unit. This is important for the practical execution of a vacuum swing to regenerate the sorbent. However, SARC reactors must be operated dynamically, which requires a cluster of reactors operated in a coordinated manner to act as a steady-state processing unit. A heat pump is used to continuously transfer heat from the reactors in the carbonation and cooling steps to the reactors in the regeneration step. The inclusion of a vacuum swing in the regeneration step ensures that the required temperature swing is small, thereby maximizing the efficiency of the heat pump and minimizing the energy requirement to heat and cool the sorbent and the reactor body.

Previous works have assessed the performance of the SARC concept when applied to a coal-fired power plant (Zaabout et al., 2017), finding a promising energy penalty as low as 8 %-points (Cloete et al., 2018). The more concentrated CO_2 stream produced by a cement plant is expected to further reduce the SARC energy consumption due to the smaller temperature and pressure swings required to achieve a specified fraction (90%) of CO_2 capture. This study will therefore replicate the previous work on a coal-fired power plant for application to a cement plant, where the main differences consist in flue gas richer in CO_2 and in the lack of a steam cycle that can recover the excess heat generated within the SARC process. The results will then be benchmarked against several competing processes to thoroughly assess the potential of the SARC concept for application to cement production.

2. Reactor simulations

Reactor simulations were identical to those detailed in Cloete et al. (2018), using CO_2 and H_2O adsorption isotherms from Veneman et al. (2015) as detailed in Zaabout et al. (2017). A summary of the model setup will be provided below for ease of reference, but the reader is referred to the aforementioned works for further details.

2.1. Reactor model

The SARC reactor was modelled as four continuously stirred tank

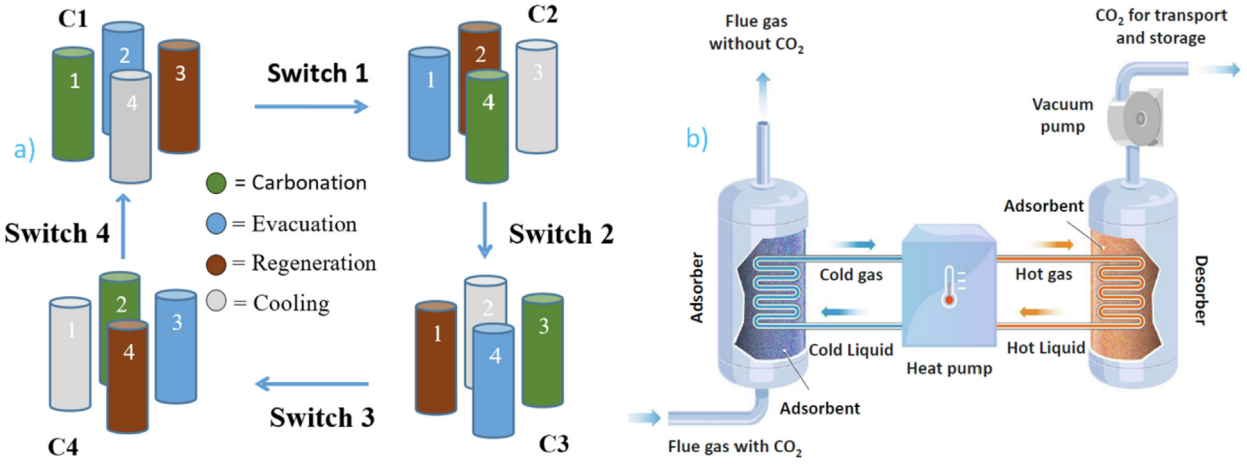

Fig. 1. SARC conceptual design: a) a cluster of SARC reactors for continuous gas stream processing; b) SARC working principle showing heat transfer from a reactor under carbonation to one under regeneration using a heat pump. Reprinted from Cloete et al. (2018), page 2, Copyright (2019), with permission from Elsevier.

reactors (CSTR) in series (acting as a four-stage fluidized bed reactor) as described in detail in Zaabout et al. (2017). The model is solved using the ode15s solver in MATLAB. The four SARC process steps outlined in the introduction are performed sequentially in the transient reactor model with the target of achieving 90% CO_2 capture and 96% CO_2 purity. Multiple such transient cycles are completed with a simple feedback controller adjusting the heat pump condensation temperature (the amount of temperature swing) to achieve 90% CO_2 capture and the evacuation pump extraction rate to achieve 96% CO_2 purity. Once these targets are reached, the transient outlet streams from each step are averaged and this stream data is passed to the process modelling, in addition to the amount of heat transferred by the heat pump, the heat pump condensation and evaporation temperatures, and the vacuum pressure required in the evacuation step to achieve the desired level of CO_2 purity.

Chemical and thermal equilibrium is assumed inside the reactors. Thermal equilibrium is generally a good assumption in fluidized beds, but the chemical equilibrium assumption requires more detailed study including reaction kinetics, which are currently not available under the vacuum conditions employed in the SARC concept. The large and dense fluidized bed reactors employed in this study increase the validity of this assumption by increasing the contacting time and available surface area for reaction inside the reactor.

The multi-stage configuration of the SARC reactor ensures that the gas-solid contacting proceeds more as a plug flow reactor (PFR) than a complete CSTR. Previous work showed that four CSTRs in series captures most of the benefits of PFR flow behaviour (see Fig. 6 in Zaabout et al. (2017)). Although performance can further be improved by putting more CSTRs in series, the improvement is marginal and achieving almost complete PFR behaviour in a fluidized bed reactor will be technically challenging.

In practice, the SARC reactor will not be a series of separate fluidized beds as suggested by the CSTRs in series model employed. Instead, porous partitions will be inserted into a single fluidized bed reactor to minimize axial solids mixing. Openings in these partitions will be large enough for particles to easily pass through so that no blockage can take place, but still small enough to prevent large clusters of particles from falling freely at the walls and forming the large-scale recirculation patterns typical in bubbling fluidized beds. The presence of the dense array of heat transfer tubes in the reactor will also minimize back-mixing, making the fluidized bed reactor behave more like a PFR. The choice of the number of CSTRs in series is therefore an indication of the degree of back-mixing prevention through the aforementioned mechanisms (zero back-mixing would result in PFR behaviour and infinite back-mixing would result in a single CSTR). The selection of four CSTRs is seen as an intermediate value that delivers most of the benefits and should still be achievable in practice.

For this study, a cluster of 25 SARC reactors was employed. Each reactor is 3.46 m in diameter and 6.92 m in height (aspect ratio of 2). At any given time, 10 of these reactors are in carbonation. The reactors were sized so that the fluidization velocity in carbonation is 1 m/s under the conditions given in Table 3 (Stream 1). The three remaining process steps are distributed as follows: 1 reactor for evacuation, 12 reactors for regeneration and 2 reactors for cooling. Heat is extracted from the reactor by the heat pump during carbonation and cooling and added during regeneration. This distribution therefore ensures that heat is always being extracted from 12 reactors and added to 12 reactors.

The behaviour of a single reactor operating in this manner is shown in Fig. 2. It is observed that the temperature is almost constant over the carbonation step as the sorbent is gradually carbonated and the heat pump continuously extracts the heat from this exothermic reaction. The carbonation step is stopped when the CO_2 concentration at the outlet starts to increase significantly to maintain 90% CO_2 capture. During the short evacuation stage, no flow enters the reactor and some of the N_2-rich gases are extracted, thus lowering the reactor pressure. This is done to minimize the negative effect of N_2 in the system on the purity of the CO_2 extracted in the subsequent regeneration step.

During regeneration, the pressure is reduced further to the point where the sorbent starts to release CO_2. Fig. 2 Shows that the pressure initially goes down to about 0.3 bar and then gradually reduces to the final regeneration pressure of 0.1 bar. This gradual pressure decrease is caused by a 0.1 kmol/s limit imposed on the release rate of the CO_2. Such a limit is needed in the model to prevent a large amount of CO_2 to be released instantaneously when the vacuum is drawn because such a CO_2 release will cause particle elutriation and will also be limited by regeneration kinetics. The constant CO_2 release causes a gradual decrease in the degree of carbonation of the sorbent (q_{CO_2} in Eq. (1)), which modifies the equilibrium CO_2 concentration and requires gradually stronger vacuums and higher temperatures to achieve further regeneration. When the pressure reaches 0.1 bar, all further regeneration must be driven by a temperature increase from the heat pump. Finally, the cooling step uses the heat pump to cool the reactor to a

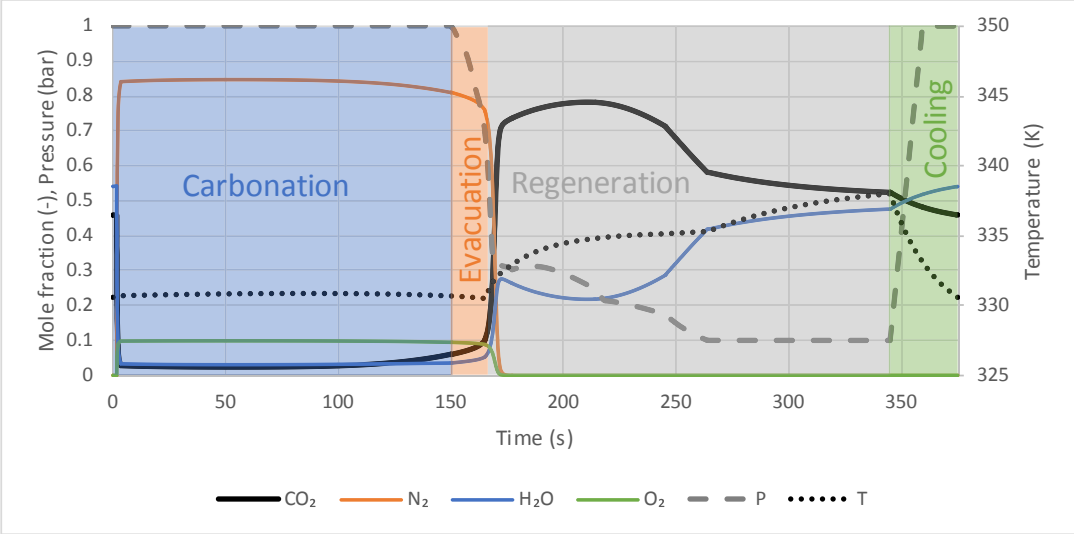

Fig. 2. Behaviour of the SARC reactor over a single cycle.

temperature where sufficiently high CO_2 capture will be possible in the subsequent carbonation step.

To enable the distribution of reactor steps between reactors outlined earlier, the carbonation step is 10x, the regeneration step 12x and the cooling step 2x the length of the evacuation step. To account for the behaviour of the cluster of 25 reactors from the simulation of a single reactor, the averaged outlet stream from each step is multiplied by the number of reactors in that step for implementation in the process simulations. This is a good representation of the real case where outlet streams from all reactors in the same step will be mixed together before being sent to downstream process units. The heat transfer tubes are assumed to be 6 mm in diameter and arranged in a staggered configuration with a pitch of 9 mm. This tube arrangement is chosen as delivering the highest practically achievable heat transfer surface area density in the reactor (a sensitivity analysis to changes in these values is presented in the results and discussion section). A square tube bundle is assumed to occupy the bottom 3.84 m of the reactor, which is also assumed to be the static bed height of the sorbent when not fluidized. This height was selected so that the bed can expand by 80% of the static bed height under fluidization before excessive particle elutriation takes place (when the bed expansion sometimes reaches the reactor outlet, leading to large losses of particles).

The heat capacity of the tube bundle and reactor body was accounted for in the simulation, increasing the amount of heat that needs to be transferred to achieve the required temperature swing. In addition, 10% of additional pressure drop to that required to fluidize the particles was assumed for the gas distributor, thus increasing the power required to feed the flue gas into the reactors.

2.2. Sorbent

A functionalized amine sorbent (Veneman et al., 2015) was employed in this simulation study. According to Veneman et al. (2015), the material was prepared by physical impregnation of Diaion® HP-20 with polyethyleneimine (PEI), which had an average molecular weight of 10,000 g/mol. The study aimed for achieving an amine loading of 35%. The final sorbent had a density of 880 kg/m^3 and a heat capacity of 1500 J/kg.K.

For CO_2 adsorption, the Toth isotherm given in Eq. (1) to Eq. (4). (Serna-Guerrero et al., 2010) was employed with the experimentally extracted parameters in Table 1 (Veneman et al., 2015). The isotherm describes the CO_2 loading of the sorbent, q_{CO_2} (mol/kg), as a function of the CO_2 partial pressure, p_{CO_2} (bar), and the temperature, T (K).

$$q_{CO_2} = \frac{n_s b p_{CO_2}}{\left(1 - (b p_{CO_2})^t\right)^{\frac{1}{t}}} \tag{1}$$

$$b = b_0 \exp\left(\frac{\Delta H}{R T_0}\left(\frac{T_0}{T} - 1\right)\right) \tag{2}$$

$$n_s = n_{s,0} \exp\left(X\left(1 - \frac{T}{T_0}\right)\right) \tag{3}$$

$$t = t_0 + \alpha\left(1 - \frac{T_0}{T}\right) \tag{4}$$

For H_2O adsorption, the following model was fitted (Zaabout et al., 2017) from the data provided by Veneman et al. (2015). The H_2O loading on the sorbent, q_{H_2O} (mol/kg), is described by a simple polynomial as a function of the relative humidity, ϕ. $P^*_{H_2O}$ (bar) is the equilibrium vapor pressure of water.

$$q_{H_2O} = 9.01224 \times 10^{-4}\phi^2 + 2.79362 \times 10^{-2}\phi + 1.1965 \tag{5}$$

$$\phi = 100\frac{P_{H_2O}}{P^*_{H_2O}} \tag{6}$$

Table 1
Toth isotherm parameters for use in Eq. (1) to Eq. (4) (Veneman et al., 2015).

t_0	0.3
b_0	408.84 bar^{-1}
$n_{s,0}$	3.4 mol/kg
X	0
α	0.14
ΔH	86.7 × 10^3 J/mol
T_0	353 K

$$P^{*}_{H_2O} = 770529 \exp\left(\frac{-5050}{T}\right) \quad (7)$$

3. Plant simulations

The schematic of the SARC process considered in this work is shown in Fig. 3 with stream data presented in Table 3. CO_2-rich gas from the raw mill of the cement plant is compressed by a fan and fed to the reactor in the carbonation step (stream #1). This reactor is cooled by the NH_3 heat pump evaporator, which is assumed to be a drum type evaporator with forced circulation assisted by an ammonia pump. The partly evaporated ammonia at evaporator outlet (#10) is returned to the NH_3 drum, where vapor and liquid phases are separated.

Ammonia vapor from the drum (#12) is compressed by the heat pump compressor and fed to the heat pump condenser (#7), which provides heat for the SARC regeneration step. Condensed ammonia (#8) at condenser outlet is throttled and returned to the drum (#9). In the regenerator, CO_2 is released (#5) and compressed by a 3-stage intercooled compressor for pipeline transportation and permanent storage (#7). As the SARC process parameters are tuned to achieve a CO_2 purity of 96%$_{db}$, no further CO_2 purification step is assumed in addition to condensate separation after the intercoolers and dehydration (not shown in Fig. 3) before the last CO_2 compressor. Part of the CO_2 from the regenerator is recirculated to the reactor inlet (#6) for bed fluidization in the regeneration stage.

In the heat pump system, excess heat must be rejected to the ambient to close the heat balance, since the ammonia vapor generated in the carbonation step exceeds the need of the regeneration step. When SARC process is integrated in coal power plants, such heat can be recovered in a condensate preheater (Zaabout et al., 2017). In cement plants, this relatively small amount of heat (about 3 MW, corresponding to 4% of the heat absorbed in the carbonator step) is rejected to the ambient by condensation of part of the ammonia vapor (#11).

The SARC system is completed by the reactor cooling step (not shown in Fig. 3) and by the evacuation step. Gas from the evacuation step (#3) is compressed in an intercooled vacuum pump, mixed with the CO_2 lean gas from the carbonation step and emitted to the atmosphere after particle filtration.

In addition to the assumptions presented in Section 2, the other main assumptions for the calculation of the mass and energy balances of the SARC system are listed in Table 2. For the SARC unit, assumptions are consistent with previous works by the same authors (Zaabout et al., 2017). For CO_2 compression, assumptions consistent with Anantharaman et al. (2017) have been adopted.

Consistently with previous works on SARC process integration (Zaabout et al., 2017), the in-house code GS (Gecos, 2014) (for the heat and mass balance involving low pressure gases) and Aspen Plus (AspenTech, 2016) (for final CO_2 compression and liquefaction) software have been used for the calculations of the energy balance of the SARC system, whereas the ammonia heat pump has been calculated with an Excel spreadsheet linked with REFPROP (Lemmon et al., 2018).

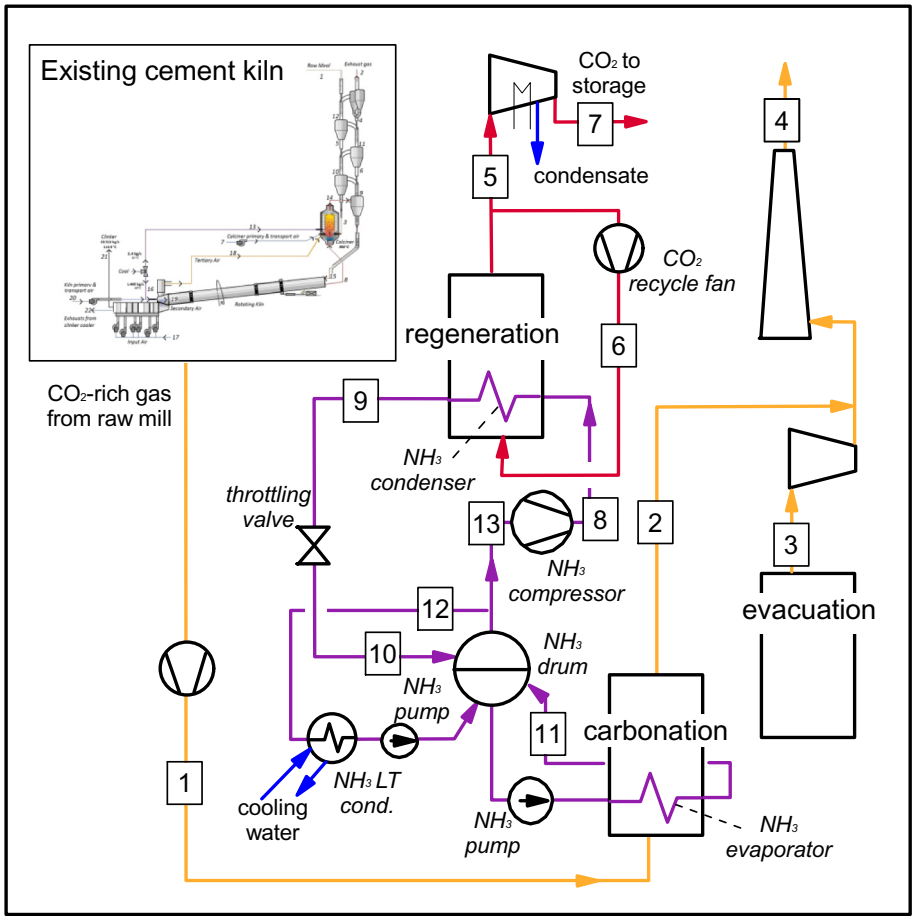

Fig. 3. Schematic of the proposed integration of the SARC process in a cement plant. The reactor under cooling step is not shown. Details of the numbered streams are given in Table 3.

Table 2
Main assumptions for the calculation of the heat and mass balances of the SARC process.

SARC PROCESS	
Heat pump compressor isentropic efficiency, %	85
Heat pump compressor electric-mechanical efficiency, %	94
Vacuum pumps isentropic efficiency, %	85
Vacuum pumps electrical-mechanical efficiency, %	95
Vacuum pumps intercooling temperature, °C	35
Regenerator recycle fan isentropic efficiency, %	80
Regenerator recycle fan electrical-mechanical efficiency, %	94
Pressure loss in gas distribution nozzles, % of solid inventory weight	10
CO_2 COMPRESSION	
Compressors isentropic efficiency, %	85
Compressor electrical-mechanical efficiency, %	95
Number of compressor stages	4
Intercoolers outlet temperature, °C	35
After-cooler outlet temperature, °C	25
Pump isentropic efficiency, %	80
Pump electrical-mechanical efficiency, %	95
Pumping pressures start/delivery, bar	80/110

Table 3
Properties of the main streams referring to Fig. 3 for the base case considered in this study (carbonation time of 150 s and regeneration pressure of 0.1 bar).

Stream	T, °C	p, bar	ṁ, kg/s	Mole fraction, %				
				CO_2	H_2O	N_2	O_2	NH_3
1	60	1.19	88.39	22.49	11.44	59.53	6.54	
2	60	1.01	55.69	3.13	3.59	84.12	9.17	
3	60	0.70	1.76	7.37	4.13	79.25	9.25	
4	60.4	1.01	57.45	3.23	3.58	84.00	9.19	
5	62.0	0.10	30.94	67.45	29.74	2.52	0.29	
6	85.5	0.13	3.44	67.45	29.74	2.52	0.29	
7	25	110	26.31	96.0		3.6	0.4	
8	76.4	29.94	72.57					100
9	65.6	29.94	72.57					100
10	55	23.02	72.57					100
11	55	23.02	75.64					100
12	55	23.02	3.08					100
13	55	23.02	72.57					100

4. Results and discussion

Results will be presented in five sections:

1. An illustration of the SARC reactor behaviour.
2. The influence of heat integration with the cement plant on the SARC energy demand. Integrating waste heat from the cement plant will reduce the power consumption of the heat pump, lowering the energy penalty.
3. The effect of two important operating parameters; regeneration pressure and cycle length, on the SARC energy demand. Increasing the regeneration pressure will exchange lower vacuum pump power consumption for higher heat pump power consumption. Longer cycle lengths will reduce the amount of heat transfer required to heat and cool the particles in exchange for a larger difference between condensation and evaporation temperatures, creating a trade-off between the amount of heat transfer and the efficiency of the heat pump.
4. The effect of two important design parameters; tube arrangement and reactor size, on the SARC energy demand. Increasing the area density of the heat transfer surfaces or increasing the size of the reactor (at a constant area density) will reduce the temperature difference between the reactor and the heat transfer fluid, increasing heat pump efficiency in exchange for a more expensive reactor.
5. Benchmarking of the SARC performance against several competing technologies, including calcium looping, amine solvents and oxyfuel.

4.1. SARC reactor behaviour

The qualitative behaviour of the SARC concept in a cement plant is similar to that previously reported for a coal plant (Zaabout et al., 2017). Quantitative differences arise because the flue gas composition of the cement plant contains a higher concentration of CO_2 (22%) than the coal plant (13.4%). This means that the SARC reactor needs less temperature and/or pressure swing to achieve the same fraction of CO_2 capture (90%). This quantitative difference is illustrated in Fig. 4, where the coal plant flue gas was approximated by simply reducing the CO_2 concentration to 13.4% and increasing the N_2 concentration to ensure that the species sum to unity.

Since the pressure swing was kept constant between these two cases, the difference is only apparent in the temperature swing. Clearly, the temperature swing required for the cement flue gas (Fig. 4, top) is significantly smaller than for the coal power plant flue gas (Fig. 4, bottom). This difference originates because the CO_2 partial pressure in the carbonation stage outlet gas can be higher in the case of the cement flue gas than the coal plant flue gas (to achieve the target CO_2 capture efficiency of 90%). The power consumption of the cement plant SARC can therefore be expected to be significantly lower than that of the coal power plant SARC.

4.2. Heat integration

In cement plants, some heat can be recovered to reduce the heat demand of the CO_2 capture unit. The amount of waste heat available depends on the thermal efficiency of the cement kiln and on the heat needed for raw meal drying. In the high-efficiency reference cement kiln, with an assumed raw material initial moisture of $6\%_{wt.}$ (Anantharaman et al., 2017), about 5 MW (or 150 kJ per kg of clinker) is available by cooling the excess air from the clinker cooler to 100 °C.

Fig. 5 shows that the positive effect of integrating the waste heat from the cement plant into the SARC process is small. A non-negligible (11.4%) reduction in heat pump power consumption is achieved via heat integration, but, since the heat pump consumption is a relatively small fraction of the overall power consumption, the total energy saving from heat integration is only 1.3%. For this reason, the remainder of the cases in this paper will be presented for the case with no heat integration.

As a rough quantification of the reduction in energy consumption for the cement plant SARC relative to the coal plant SARC, it can be noted that the ratio of total power consumption to CO_2 compression in this case is 2.3, whereas this ratio was 2.9 for the coal plant previously assessed using the same sorbent (Zaabout et al., 2017). This shows the substantial reduction in combined heat and vacuum pump consumption allowed by the higher CO_2 concentration in the flue gas.

It should be noted, however, that older and less efficient cement plants have much larger quantities of heat available for integration into the SARC process. Future studies into the retrofitting of older plants with SARC technology will therefore revisit the potential of heat integration to further reduce the energy penalty. Heat integration will also reduce costs related to the heat pump compressor, but it will require an additional heat exchanger in the system. This trade-off will be investigated in future economic analyses of the SARC concept.

4.3. Operating parameters

SARC reactor performance is particularly sensitive to two

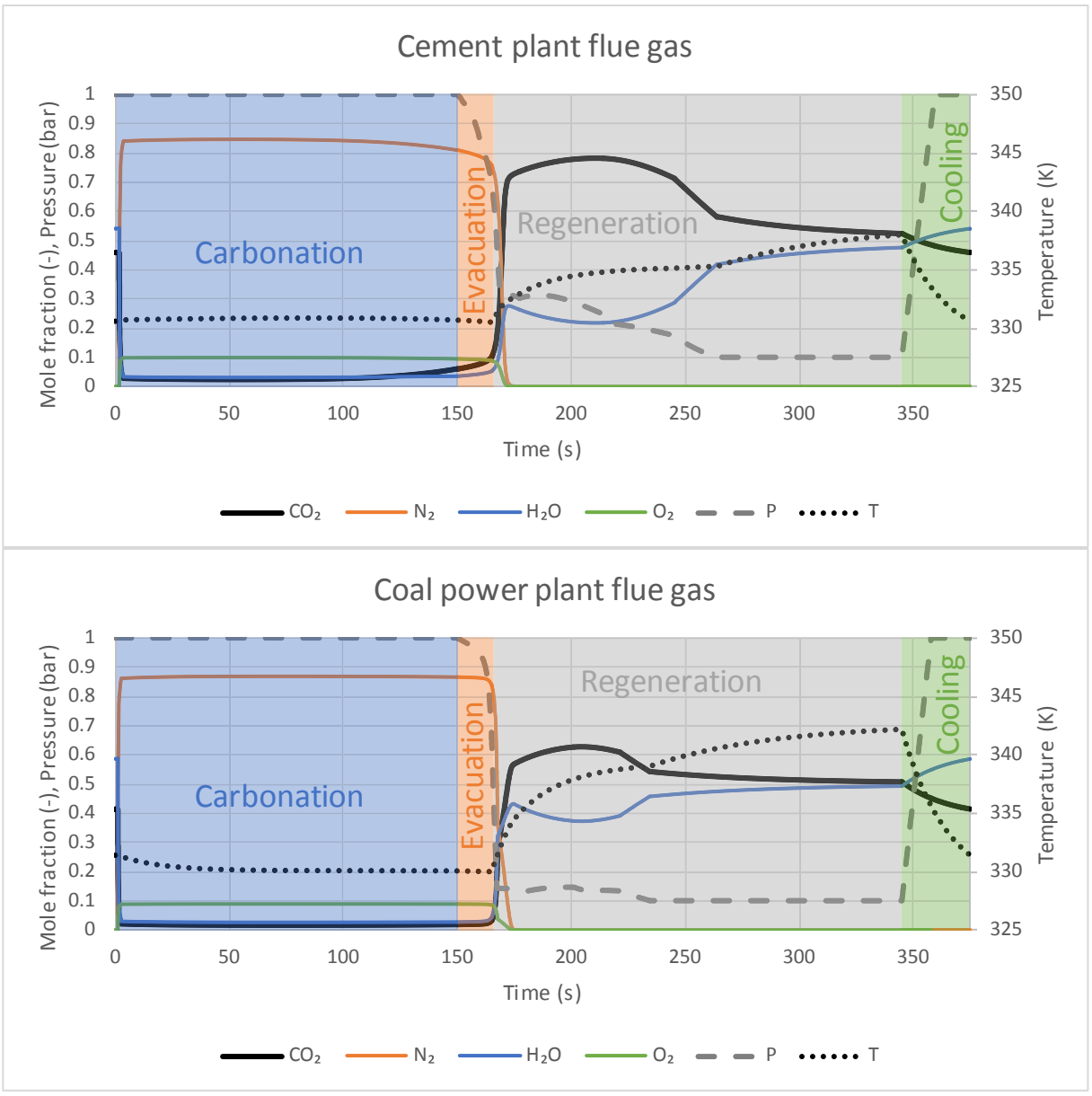

Fig. 4. Gas species mole fractions, reactor pressure and reactor temperature over one SARC cycle for a flue gas containing 22% CO_2 (top) and a flue gas containing 13.4% CO_2 (bottom).

operating parameters: the amount of pressure swing and the cycle time. A large pressure swing (stronger vacuum drawn in the regeneration step) will allow for a smaller temperature swing to achieve a set CO_2 capture ratio, thereby increasing the heat pump efficiency and lowering the sensible heat required to heat and cool the sorbent and the reactors.

For a coal-fired power plant, it was found that the regeneration pressure should be as low as practically possible (0.1 bar) to minimize the energy penalty (Cloete et al., 2018). Webley (2014) reported that even these vacuums will be challenging due to the large required vacuum pump sizes and associated scalability concerns. Based on this information, the effect of increasing the regeneration pressure to 0.2 bar will be investigated.

A change in the cycle time will change the degree of sorbent carbonation achieved in each cycle. A shorter cycle will require a smaller change in CO_2 loading of the sorbent, thereby allowing for a smaller temperature swing and a more efficient heat pump. On the other hand, shorter cycles impose a larger sensible heat requirement per unit of captured CO_2. Each temperature swing requires the sorbent and the reactor to be heated and cooled via heat transfer through the heat pump. Short cycles will capture less CO_2 for each temperature cycle, thereby increasing the amount of heat transfer required.

As can be seen in Fig. 6 (left), an increase in regeneration pressure from 0.1 bar to 0.2 bar causes a substantial (14.5%) increase in total electricity consumption. As the regeneration pressure is increased, the vacuum pump consumption decreases, but this positive trend is more than cancelled out by increasing heat pump consumption. A larger required temperature swing both decreases heat pump efficiency and increases the sensible heat requirement for heating and cooling the sorbent and reactor for each cycle. Based on this finding, the rest of the study will be carried out at a regeneration pressure of 0.1 bar. Future economic assessment work will be needed to see if the higher efficiency and less powerful heat

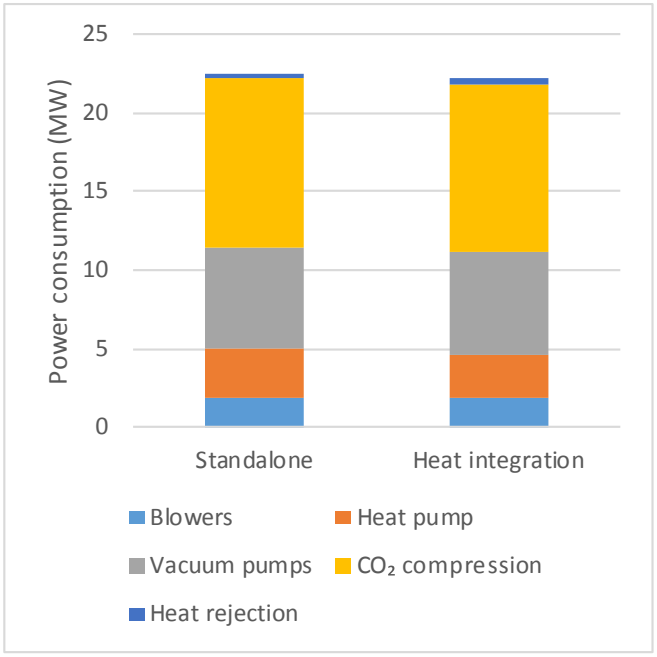

Fig. 5. Breakdown of SARC electricity consumption for cases with and without heat integration.

pump compressor can justify the large vacuum pump required for the 0.1 bar case.

Fig. 6 (right) shows an optimal energy consumption at a carbonation time of 150 s. This equates to a total cycle time of 375 s, given that 10 out of the 25 reactors are in carbonation at any given time. In this case, the heat pump consumption represents the only significant change between the different cases. If the carbonation time is increased above 150 s, the larger temperature swing required increases the overall heat pump consumption. If the carbonation time is decreased below 150 s, the larger sensible heat requirement increases the overall heat pump consumption. These conflicting effects are optimally balanced at 150 s carbonation time, which will be used in the rest of the study.

4.4. Design parameters

The amount of heat transfer surface area available inside the SARC reactor is an important factor in determining the heat pump efficiency. If the heat transfer surface area is smaller, a larger temperature difference between the heat pump working fluid and the sorbent is required to achieve the required heat transfer rate. This increases the required difference between the condensation and evaporation temperatures of the working fluid, reducing the heat pump efficiency.

The heat transfer surface area can be increased by simply increasing the reactor size. However, aside from increasing the reactor capital cost, a taller reactor will also increase the pressure drop over the reactor, increasing the power consumption required to feed the flue gas to the reactor. Alternatively, the heat transfer tubes can be made smaller and positioned more closely together to increase the available heat transfer area per unit reactor volume. This will have some reactor cost trade-offs to be assessed in a future economic assessment, but will not influence the reactor pressure drop or footprint.

Fig. 7 shows the trends in SARC power consumption with a change in tube diameter and reactor volume (at a fixed reactor aspect ratio of 2). As expected, the heat pump consumption reduces with a decrease in tube diameter and an increase in reactor volume, both of which will increase the available heat transfer area, thereby reducing the required heat pump temperature difference. In the case of increasing reactor volume, this trend is partially counteracted by increasing power consumption of the flue gas blower required to overcome the reactor pressure drop. Overall efficiency gains beyond the base case (100% reactor volume in Fig. 7, right) are therefore minimal.

The heat transfer per unit reactor volume can be increased in other ways than reducing the tube diameter. Data from Fig. 7 (left) was used to explore these options through Fig. 8. Here, the four cases in Fig. 7 (left) were used to calculate the volumetric heat transfer coefficient using the assumed heat transfer coefficient of 300 W/m^{2}K. Fig. 8 investigates four different ways to manipulate

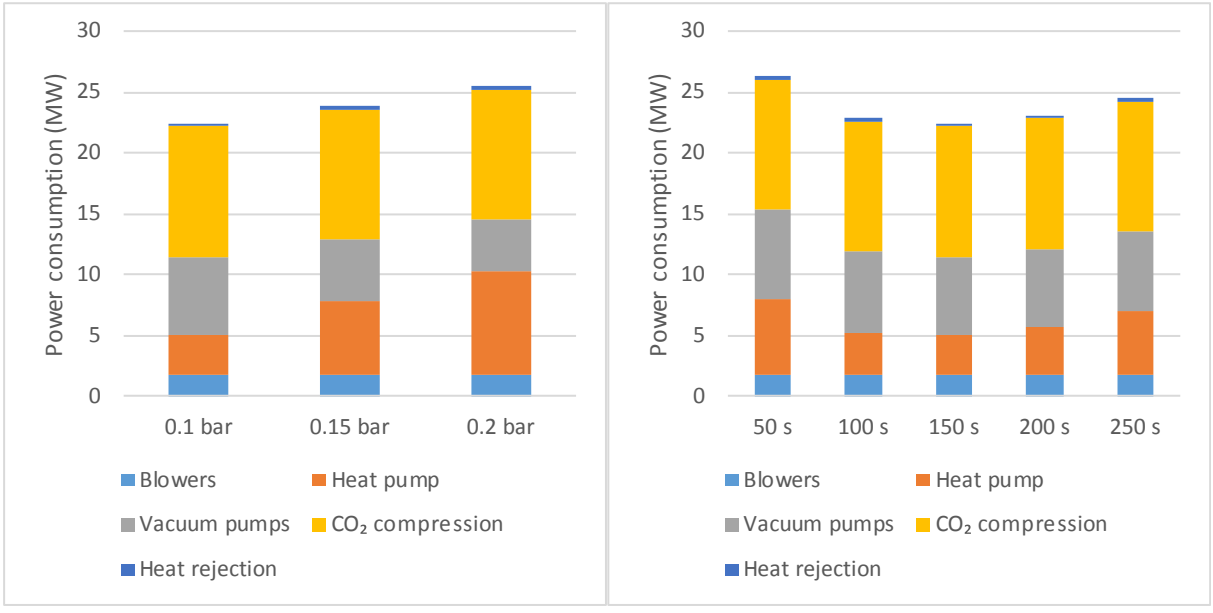

Fig. 6. The effect of regeneration pressure at a 150 s carbonation time (left) and carbonation time at a regeneration pressure of 0.1 bar (right) on SARC electricity consumption.

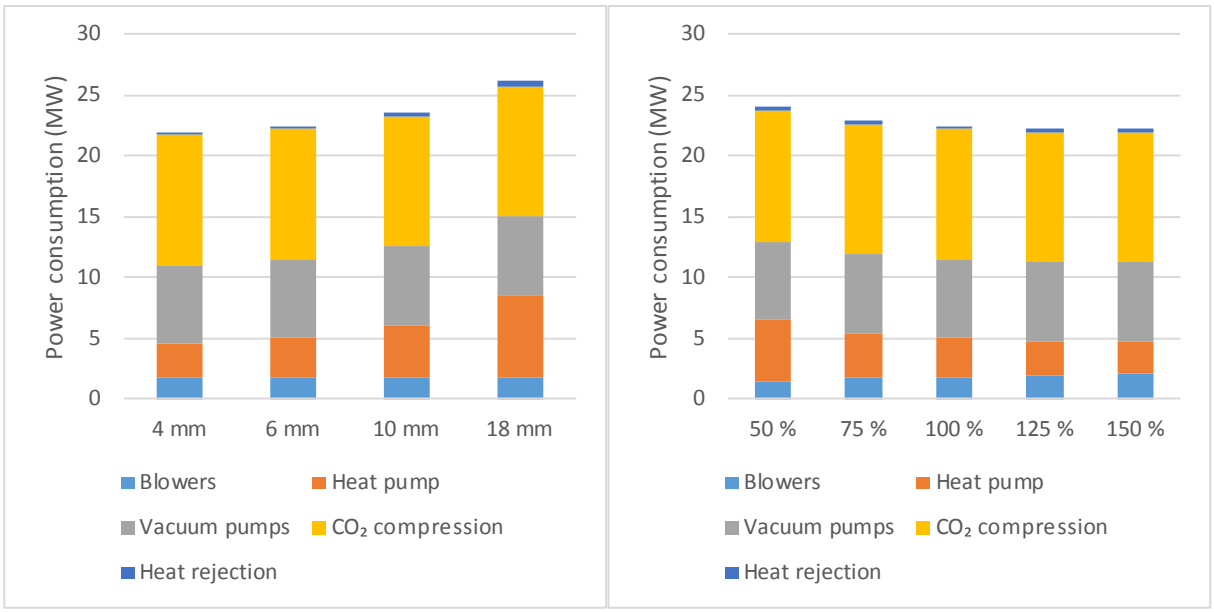

Fig. 7. The effect of heat transfer tube diameter (left) and overall reactor volume as a percentage of the base case (right) on SARC electricity consumption.

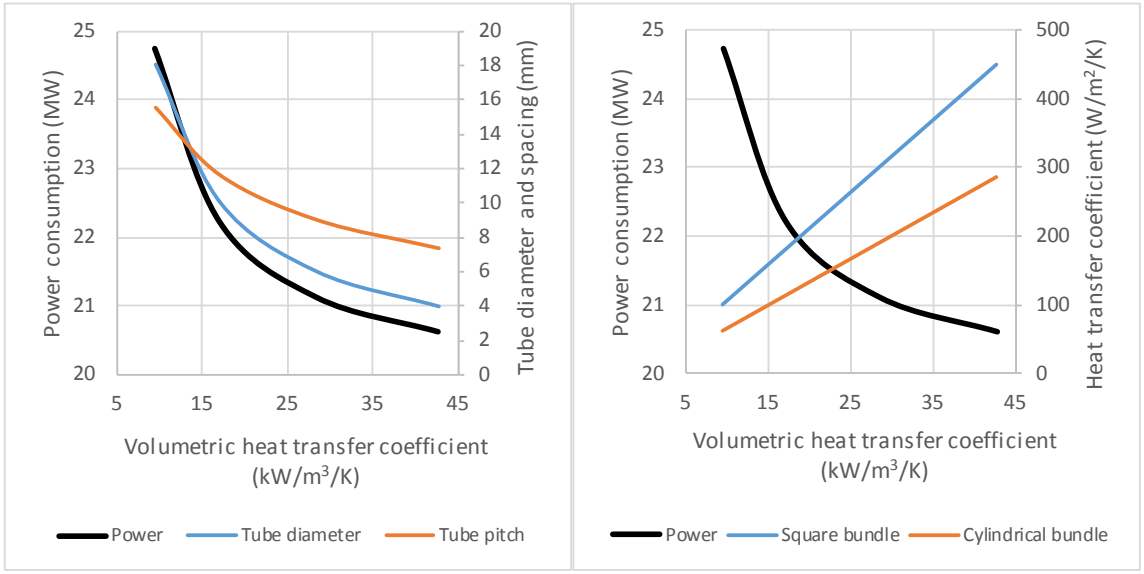

Fig. 8. The volumetric heat transfer coefficient can be increased by decreasing the tube diameter or tube pitch (left) or by increasing the bed-to-tube heat transfer coefficient and installing a cylindrical tube bundle (right). Both graphs show the decrease in SARC power consumption with increased volumetric heat transfer coefficient.

the achieved volumetric heat transfer coefficient:

1. Changing the tube diameter as in Fig. 7 (left). Note that the ratio of tube pitch to tube diameter was kept constant at 1.5 for all the cases.
2. Changing the tube pitch (spacing between the centres of the staggered tubes). In this case, the tube diameter was kept constant at 6 mm.
3. Changing the heat transfer coefficient for a tube diameter of 6 mm and a pitch of 9 mm.
4. Changing from a square tube bundle to a cylindrical tube bundle that covers the entire cross-sectional area of the cylindrical reactor.

The first observation from Fig. 8 is that the reduction in power consumption achieved by further increases in the volumetric heat transfer coefficient beyond the base case (28.5 kW/m^{3}K) are small. In the base case, the temperature difference between the reactor and the working fluid is already only about 2.7 K, leaving little room for further improvement. When the volumetric heat transfer coefficient is decreased below the base case, however, the energy consumption increases at an accelerating rate as each halving of the volumetric heat transfer coefficient requires a doubling of the temperature difference between the reactor and the working fluid.

Further economic assessment work will be required to evaluate the trade-off between increased heat transfer surface area and decreased heat pump power consumption. As an initial indication, it can be noted that the heat transfer surface area inside the reactor

for the base case is 6189 m^2 and was varied between 2062 and 9283 m^2 in Fig. 8. These large heat transfer areas will impose a substantial cost that should be weighed against the electricity savings and reduced heat pump compressor cost that will result from larger heat transfer areas.

It is interesting to note from Fig. 8 (left) that the tube pitch (at a constant tube diameter) has a larger influence on the volumetric heat transfer coefficient than the tube diameter (at a constant pitch/diameter ratio). Tubes should therefore be positioned as close together as practically possible.

Fig. 8 (right) shows the relationship between the volumetric and surface area heat transfer coefficients. This study and the previous SARC studies in a coal power plant assumed a heat transfer coefficient of 300 W/m^2K based on experimental observations (Kim et al., 2003). However, the heat transfer coefficient depends on many factors, including the tube size and arrangement, the fluidization velocity and particle properties. It therefore represents an important uncertainty in the assessment of the SARC heat pump efficiency. For example, if the actual heat transfer coefficient was 200 W/m^2K instead of 300 W/m^2K, the total SARC power consumption would increase by about 4%.

The use of a cylindrical tube bundle filling the entire cross-sectional area of the reactor will increase the available surface area by a factor of $\pi/2 = 1.57$ and will therefore have a slightly larger positive effect than an increase in the heat transfer coefficient from 200 W/m^2K to 300 W/m^2K. Such a tube bundle will be more challenging to manufacture than a square tube bundle, but the large increase in available surface area may be worth this added manufacturing complexity. It may also be that a tube bundle covering the entire cross-sectional area is important to further restrict axial mixing to ensure that the reactor behaves more like a PFR than a CSTR.

4.5. Benchmarking

Detailed mass and energy balance indicators of the cement kiln integrated with the SARC process are reported in Table 4. In the SARC CO_2 capture plant, most of the power is consumed for CO_2 compression (47% of the total), followed by the vacuum pump (29%). The heat pump compressor consumes a relatively low electric power of 3.14 MW_e, corresponding to 14% of the total. The total electricity consumption of the SARC system is 186.4 kWh/t_{clk}, leading to a total power consumption of the cement kiln integrated with the SARC process of 318 kWh/t_{clk} (140% more than the reference kiln without CO_2 capture).

Following the CEMCAP benchmarking methodology (Anantharaman et al., 2017), the overall balance includes the effect of the indirect fuel consumption and CO_2 emission associated to the electric power consumed by the cement plant. The reference CEMCAP power generation scenario (electric efficiency = 45.9%, CO_2 emission = 262 kg/MWh) has been assumed in the calculations, corresponding to the EU-28 mix of year 2014. The equivalent (i.e. direct + indirect) primary energy consumption ($q_{clk,\,eq}$) and CO_2 emission ($e_{clk,eq}$) have been calculated for both the reference cement kiln without capture and the kiln with CO_2 capture by SARC process. The equivalent primary energy consumption and the equivalent CO_2 emissions resulted 35% higher and 81% lower than the reference cement kiln without capture.

The equivalent quantities are used to calculate the specific primary energy consumption for CO_2 avoided (SPECCA), according to Eq. (8), leading to a value of 2.04 MJ_{LHV}/kg_{CO2}. The obtained SPECCA value is competitive compared with the other CO_2 capture technologies for cement plants. According to the CEMCAP project results (Voldsund et al., 2019), only oxyfuel technology has a lower SPECCA (1.63 MJ_{LHV}/kg_{CO2}), while all the other assessed technologies (MEA, chilled ammonia, calcium looping and membrane assisted liquefaction) showed a SPECCA higher than 3 MJ_{LHV}/kg_{CO2} (Fig. 9).

Table 4
Mass and energy balance indicators for the cement kiln integrated with the SARC process (base case: carbonation time = 150 s, regeneration pressure = 0.1 bar, tube diameter = 6 mm, reactor height = 6.92 m, heat transfer coefficient = 300 W/m^2K). Indirect primary energy consumptions and CO_2 emissions are calculated with an electric efficiency = 45.9% and CO_2 emission = 262 kg/MWh (reference CEMCAP power generation scenario (Anantharaman et al., 2017)).

Cement kiln	
Clinker production, tpd	2896
Cement production, tpd	3929
CO_2 generated, kg/s	28.5
kg/t_{clk}	850
kg/t_{cem}	626
Fuel consumption, MW_{LHV}	105
kJ_{LHV}/kg_{clk}	3135
kJ_{LHV}/kg_{cem}	2311
Electric power consumption, MW	15.9
kWh/t_{cem}	97
kWh/t_{clk}	131.6
SARC plant (base case)	
Power absorption, MW_e	
Carbonator fan	1.77
Regenerator recycle fan	0.09
Vacuum pump	6.44
Evacuation vacuum pump	0.07
Heat pump compressor	3.14
CO_2 compression	10.68
Auxiliaries for heat rejection	0.30
Total power consumption, MW_e	22.49
kWh/t_{clk}	186.4
CO_2 captured, kg/s	25.65
Direct CO_2 emission, kg/s	2.85
kg/t_{clk}	85.0

Overall balance	Plant without capture	Plant with CO_2 capture
Total electric consumption, kWh/t_{clk}	131.6	318.0
Indirect primary energy consumption, kJ_{LHV}/kg_{clk}	1032	2494
Equivalent primary energy consumption, kJ_{LHV}/kg_{clk}	4167	5629
Indirect CO_2 emissions, kg/t_{clk}	34.5	83.3
Equivalent CO_2 emissions, kg/t_{clk}	884.5	168.3
CO_2 avoided, %		81.0
SPECCA, MJ_{LHV}/kg_{CO2}		2.04

$$SPECCA = \frac{q_{clk,\,eq} - q_{clk,eq,ref}}{e_{clk,eq,ref} - e_{clk,eq}} \quad (8)$$

Given that the SARC plant consumes only electricity, the power generation mix has a large impact on the SPECCA of the plant. For example, in a 100% renewable electricity scenario (electric efficiency = 100%, CO_2 emission = 0 kg/MWh), the SPECCA reduces to only 0.88 MJ_{LHV}/kg_{CO2}, whereas the SPECCA increases to 2.66 MJ_{LHV}/kg_{CO2} in a coal-dominated electricity mix (average fossil power mix of EU-28 in 2014 (Anantharaman et al., 2017): electric efficiency = 40.6%, CO_2 emission = 776 kg/MWh). It is therefore clear that SARC is best suited to regions where the electricity sector has already achieved a relatively high level of decarbonization.

In addition to the low SPECCA, the SARC process has the significant advantage of being a post-combustion capture technology that does not affect the cement production process and does not require additional fuel or steam for sorbent regeneration, but only requires electricity to run the compressors. This will simplify the retrofitting of existing cement plants with this CO_2 capture process.

The main drawback is related to the high footprint required (about 235 m^2), due to the relatively low gas velocity (1 m/s) in the

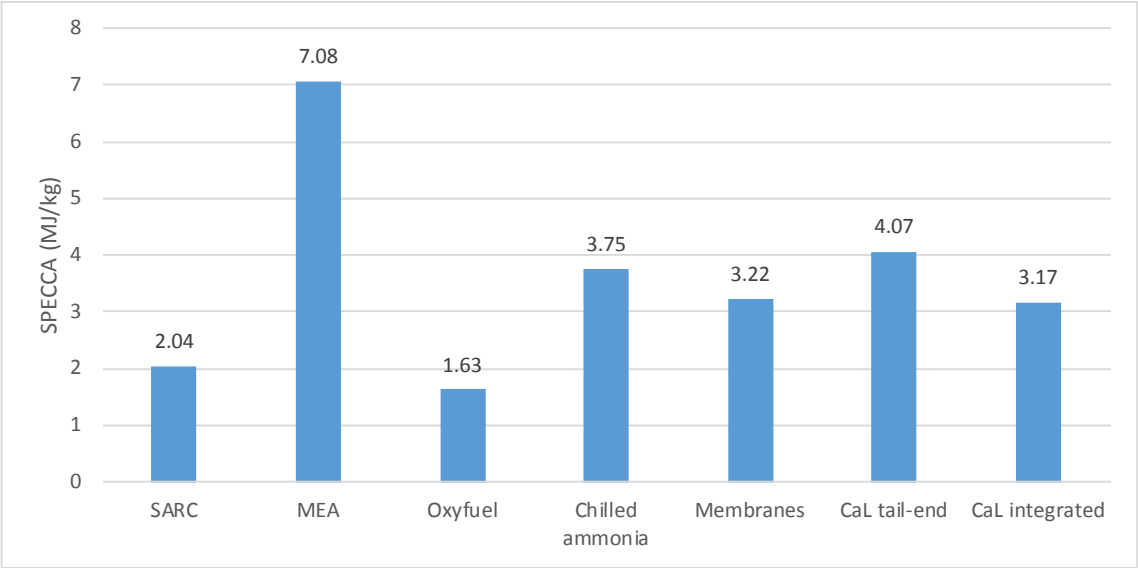

Fig. 9. Comparison of SPECCA values for SARC with different technologies investigated in the CEMCAP project (Voldsund et al., 2018). The reference CEMCAP power generation scenario (electric efficiency = 45.9%, CO_2 emission = 262 kg/MWh) was used for all technologies that consume electricity.

reactors in the carbonation step and to the presence of more reactors in the regeneration, evacuation and cooling steps than those in the carbonation step. As a result of this low flowrate, the reactor height is small relative to other CO_2 capture systems (about 7 m), implying that the footprint could be reduced by stacking several reactors on top of each other if required. It must also be mentioned that the SARC concept has only been demonstrated at bench scale (Dhoke et al., 2018) and the tolerance of the sorbent material to the impurities in the cement plant kiln gas is not known.

4.6. Implications for theory and practice on cleaner production

The combined benefits of low energy penalty and easy retrofitting makes SARC an attractive technology option for cleaner production from existing sources of CO_2 emissions. If the world eventually commits to a 1.5–2 °C global temperature rise, rapidly rising CO_2 prices will exert large economic pressures on existing fossil fuel infrastructure and other CO_2 emission sources, potentially leading to large investment losses. A technology like SARC can add great value in this scenario.

Since SARC requires no integration with the host process, it is also highly versatile to emissions abatement from a range of CO_2 emitting power plants and industries. Energy consumption for capturing 90% of emissions decreases significantly with increasing flue gas partial pressure, implying that more concentrated CO_2 sources, such as cement, should be prioritized. However, as CO_2 prices keep rising over time, more dilute CO_2 sources will become profitable as well.

5. Summary and conclusions

This study investigated the performance of the swing adsorption reactor cluster (SARC) for post-combustion CO_2 capture from a cement plant. SARC employs a synergistic combination of temperature swing (using a heat pump) and pressure swing (using a vacuum pump) to capture CO_2 via solid sorbents using electrical power only.

Compared to earlier work for integration to a coal power plant, the energy penalty of SARC decreased significantly because of the higher CO_2 fraction in the cement plant flue gas. A higher CO_2 partial pressure in the flue gas allowed for a significant decrease in the temperature swing required to achieve the fixed 90% CO_2 capture ratio, leading to a significant increase in heat pump efficiency. It can therefore be concluded that SARC is best suited to applications where the flue gas CO_2 content is relatively high.

Sensitivity analyses showed that the SARC regeneration pressure should be as low as practically possible (0.1 bar) to minimize the energy penalty. The energy penalty can be marginally reduced by increasing the heat transfer surface area inside the reactor (e.g. thinner heat transfer tubes), but this improvement must be weighed against the added reactor capital costs of such an arrangement.

Additional heat integration with the cement plant gave a negligible efficiency improvement, implying that the SARC system can be constructed as a standalone system next to the cement plant. Such a standalone SARC facility will not have any impact on the cement plant, making it ideal for retrofitting applications.

The only concern is space requirement, where the SARC reactor footprint is about 235 m^2 for capturing 90% of CO_2 emissions from a 3929 tpd cement production facility. The height of the reactors is relatively low, however, suggesting that reactors can be stacked to reduce the footprint. Another important uncertainty is the tolerance of the sorbent to impurities in the cement plant flue gas. Experimental trials with realistic flue gases are therefore recommended for future work.

A benchmarking study showed attractive energy efficiency for SARC, returning a SPECCA of 2.04 MJ_{LHV}/kg_{CO2} when using electricity from the European grid. Oxyfuel is the only technology showing a lower SPECCA (1.63 MJ_{LHV}/kg_{CO2}), but oxyfuel CO_2 capture will require substantial modifications to the cement plant. Other technologies have SPECCA values higher than 3 MJ_{LHV}/kg_{CO2}.

Given that SARC uses electricity only, the source of the electricity is important for overall energy efficiency and CO_2 avoidance. In general, SARC performs best in an electricity sector that has already achieved a high degree of decarbonization. Given the trend of reducing CO_2 intensity in most regions globally, SARC energy efficiency (as measured by SPECCA) will progressively improve over time.

Future work will complete a thorough economic assessment and benchmarking for SARC as applied to a cement plant. In

particular, the trade-offs between efficiency and capital costs relating to the regeneration pressure (size of the vacuum pump), the heat transfer surface area and the reactor size will be investigated to find the optimum CO_2 avoidance cost, which will be benchmarked against all relevant alternative technologies.

Acknowledgement

This study was performed as part of the project entitled "Demonstration of the Swing Adsorption Reactor Cluster (SARC) for simple and cost effective post-combustion CO_2 capture", funded by the Research Council of Norway under the CLIMIT program (grant no. 268507/E20).

Nomenclature

Acronyms

CaL	Calcium looping
LHV	Lower heating value
MEA	Monoentanolamine
SARC	Swing Adsorption Reactor Cluster
SPECCA	Specific primary energy consumption for CO_2 avoided
Tpd	Tons per day

Symbols

e_{CO2}	Specific CO_2 emissions [kg/t_{clk}]
q	Specific primary energy consumption [kJ/kg_{clk}]

Subscripts

Clk	clinker
Cem	cement
Db	dry basis
E	electric
Eq	equivalent
Ref	reference

References

Anantharaman, R., Berstad, D., Cinti, G., Lena, E.D., Gatti, M., Gazzani, M., Hoppe, H., Martínez, I., Monteiro, J.G.M.-S., Romano, M., Roussanaly, S., Schols, E., Spinelli, M., Størset, S., Os, P.v., Voldsund, M., 2017. D3.2: CEMCAP Framework for Comparative Techno-Economic Analysis of CO2 Capture from Cement Plants. H2020 Project: CO2 Capture from Cement Production.

Andrew, R.M., 2018. Global CO2 emissions from cement production. Earth Syst. Sci. Data 10 (1), 195–217.

Arias, B., Alonso, M., Abanades, C., 2017. CO2 capture by calcium looping at relevant conditions for cement plants: experimental testing in a 30 kWth pilot plant. Ind. Eng. Chem. Res. 56 (10), 2634–2640.

AspenTech, 2016. Aspen One V9.1.

Carrasco, F., Grathwohl, S., Maier, J., Ruppert, J., Scheffknecht, G., 2019. Experimental investigations of oxyfuel burner for cement production application. Fuel 236, 608–614.

CEMCAP, 2018. https://www.sintef.no/cemcap.

Cloete, S., Giuffrida, A., Romano, M.C., Zaabout, A., 2018. The effect of sorbent regeneration enthalpy on the performance of the novel Swing Adsorption Reactor Cluster (SARC) for post-combustion CO2 capture. Chem. Eng. J. https://doi.org/10.1016/j.cej.2018.08.196.

De Lena, E., Spinelli, M., Gatti, M., Scaccabarozzi, R., Campanari, S., Consonni, S., Cinti, G., Romano, M.C., 2019. Techno-economic analysis of calcium looping processes for low CO2 emission cement plants. Int. J. Greenh. Gas Contr. 82, 244–260.

De Lena, E., Spinelli, M., Martínez, I., Gatti, M., Scaccabarozzi, R., Cinti, G., Romano, M.C., 2017. Process integration study of tail-end Ca-Looping process for CO2 capture in cement plants. Int. J. Greenh. Gas Contr. 67, 71–92.

Dhoke, C., Zaabout, A., Cloete, S., Seo, H., Park, Y.-k., Blom, R., Amini, S., 2018. The swing adsorption reactor cluster (SARC) for post combustion CO2 capture: experimental proof-of-principle. Chem. Eng. J. https://doi.org/10.1016/j.cej.2018.10.082.

Diego, M.E., Arias, B., Abanades, J.C., 2016. Analysis of a double calcium loop process configuration for CO2 capture in cement plants. J. Clean. Prod. 117, 110–121.

Garcia, M., 2018. Cost of CO2 Capture in the Industrial Sector: Cement and Iron and Steel Industries. IEAGHG 2018-TR03.

Gardarsdottir, S.O., De Lena, E., Romano, M., Roussanaly, S., Voldsund, M., Pérez-Calvo, J.-F., Berstad, D., Fu, C., Anantharaman, R., Sutter, D., Gazzani, M., Mazzotti, M., Cinti, G., 2019. Comparison of technologies for CO2 capture from cement production—Part 2: cost analysis. Energies 12 (3), 542.

Gecos, 2014. GS Software. www.gecos.polimi.it/software/gs.php.

Gimenez, M., Paxton, C., Wassard, H., Mogensen, O., Paubel, X., Leclerc, M., Cavagné, P., Perrin, N., 2014. The oxycombustion option. Int. Cem. Rev. 37–43.

Hills, T., Leeson, D., Florin, N., Fennell, P., 2016. Carbon capture in the cement industry: technologies, progress, and retrofitting. Environ. Sci. Technol. 50 (1), 368–377.

Hornberger, M., Spörl, R., Scheffknecht, G., 2017. Calcium looping for CO2 capture in cement plants – pilot scale test. Energy Procedia 114, 6171–6174.

Hägg, M.B., Lindbråthen, A., He, X., Nodeland, S.G., Cantero, T., 2017. Pilot demonstration-reporting on CO2 capture from a cement plant using hollow fiber process. Energy Procedia 114, 6150–6165.

IPCC, 2018. Global Warming of 1.5 °C. Intergovernmental Panel on Climate Change.

Kim, S.W., Ahn, J.Y., Kim, S.D., Hyun Lee, D., 2003. Heat transfer and bubble characteristics in a fluidized bed with immersed horizontal tube bundle. Int. J. Heat Mass Transf. 46 (3), 399–409.

Lemmon, M.O., Bell, E.W., Huber, I.H., McLinden, M.L., 2018. NIST Standard Reference Database 23: Reference Fluid Thermodynamic and Transport Properties-REFPROP, Version 10.0.

Lino, M.L., Böhm, M., Hoenig, V., Ruppert, J., Becker, S., Mathai, R., 2018. D9.1: Analysis of Oxyfuel Clinker Cooler Operational Performance. H2020 Project: CO2 Capture from Cement Production.

Nelson, T.O., Coleman, L.J.I., Mobley, P., Kataria, A., Tanthana, J., Lesemann, M., Bjerge, L.-M., 2014. Solid sorbent CO2 capture technology evaluation and demonstration at Norcem's cement plant in Brevik, Norway. Energy Procedia 63, 6504–6516.

Ozcan, D.C., Ahn, H., Brandani, S., 2013. Process integration of a Ca-looping carbon capture process in a cement plant. Int. J. Greenh. Gas Contr. 19, 530–540.

Paneru, M., Mack, A., Maier, J., Cinti, G., Ruppert, J., 2018. D8.2: Oxyfuel Suspension Calciner Test Results. H2020 Project: CO2 Capture from Cement Production.

Rodríguez, N., Alonso, M., Grasa, G., Abanades, J.C., 2008. Process for capturing CO2 arising from the calcination of the CaCO3 used in cement manufacture. Environ. Sci. Technol. 42 (18), 6980–6984.

Rodríguez, N., Murillo, R., Abanades, J.C., 2012. CO2 capture from cement plants using oxyfired precalcination and/or calcium looping. Environ. Sci. Technol. 46 (4), 2460–2466.

Serna-Guerrero, R., Belmabkhout, Y., Sayari, A., 2010. Modeling CO2 adsorption on amine-functionalized mesoporous silica: 1. A semi-empirical equilibrium model. Chem. Eng. J. 161 (1–2), 173–181.

Turrado, S., Arias, B., Fernández, J.R., Abanades, J.C., 2018. Carbonation of fine CaO particles in a drop tube reactor. Ind. Eng. Chem. Res. 57 (40), 13372–13380.

Veneman, R., Frigka, N., Zhao, W., Li, Z., Kersten, S., Brilman, W., 2015. Adsorption of H2O and CO2 on supported amine sorbents. Int. J. Greenh. Gas Contr. 41, 268–275.

Voldsund, M., Anantharaman, R., Berstad, D., Fu, C., Gardarsdottir, S.O., Jamali, A., Perez-Caivo, J.-F., Romano, M., Roussanaly, S., Ruppert, J., Stallman, O., Sutter, D., 2018. D4.6: CEMCAP Comparative Techno-Economic Analysis of CO2 Capture in Cement Plants. H2020 Project: CO2 Capture from Cement Production.

Voldsund, M., Gardarsdottir, S.O., De Lena, E., Pérez-Calvo, J.-F., Jamali, A., Berstad, D., Fu, C., Romano, M., Roussanaly, S., Anantharaman, R., Hoppe, H., Sutter, D., Mazzotti, M., Gazzani, M., Cinti, G., Jordal, K., 2019. Comparison of technologies for CO2 capture from cement production—Part 1: technical evaluation. Energies 12 (3), 559.

Webley, P.A., 2014. Adsorption technology for CO2 separation and capture: a perspective. Adsorption 20 (2), 225–231.

Zaabout, A., Romano, M.C., Cloete, S., Giuffrida, A., Morud, J., Chiesa, P., Amini, S., 2017. Thermodynamic assessment of the swing adsorption reactor cluster (SARC) concept for post-combustion CO2 capture. Int. J. Greenh. Gas Contr. 60 (Suppl. C), 74–92.